7-25-2018

An inverse Ruddlesden-Popper nitride Ca7(Li1−xFex)Te2N2 grown from Ca flux

Gang Wang
Ames Laboratory and Chinese Academy of Sciences

Soham Manni
Iowa State University and Ames Laboratory, smanni@ameslab.gov

Qisheng Lin
Iowa State University and Ames Laboratory, qslin@ameslab.gov

Patrick McVey
Iowa State University and Ames Laboratory

Robert S. Houk
Iowa State University and Ames Laboratory, rshouk@iastate.edu

See next page for additional authors

An inverse Ruddlesden-Popper nitride Ca7(Li1−xFex)Te2N2 grown from Ca flux

Abstract
Nitridoferrates containing monovalent iron ions are a class of materials of recent interest as potentially novel magnetic materials. Aiming at the exploration of nitridoferrates of calcium, we report the single crystal growth from Ca flux and crystal structure of the first member (n = 2) of a series of inverse Ruddlesden-Popper nitrides with a general formula of An−1A'2BnX3n+1, where A = Li/Fe, A' = Te, B = N, and X = Ca. Single crystal X-ray diffraction analyses indicate the crystal with a composition of Ca7(Li0.32(1)Fe0.68(1))Te2N2 and the tetragonal space group I4/mmm (a = 4.7884(1) Å, c = 25.3723(4) Å, Z = 2). The structure features alternately stacking NaCl-type A'X slabs and the perovskite-type ABX3 slabs along the c axis. The Li/Fe atoms are located in cuboctahedral cavities surrounded by eight Ca6N octahedra in the ABX3 slab. This work demonstrates the viability of the Ca-rich flux as a suitable solvent for the exploration of new complex nitrides with interesting crystal structure and properties.

Keywords
Nitrides, crystal growth, flux, crystal structure, Ruddlesden-Popper phase

Disciplines
Chemistry | Physics

Authors
Gang Wang, Soham Manni, Qisheng Lin, Patrick McVey, Robert S. Houk, Liming Wu, Sergey L. Bud'ko, and Paul C. Canfield

An inverse Ruddlesden-Popper nitride

$Ca_7(Li_{1-x}Fe_x)Te_2N_2$ grown from Ca flux

Gang Wang,[a,b,*] S. Manni,[a,c] Qisheng Lin,[a,d] Patrick McVey,[a,d] Robert S. Houk,[a,d] Liming Wu,[e] Sergey L. Bud'ko,[a,c] and Paul C. Canfield[a,c]

[1]*Ames Laboratory, Iowa State University, Ames, IA 50011, USA*

[2]*Research and Development Center for Functional Crystals, Beijing National Laboratory for Condensed Matter Physics, Institute of Physics, Chinese Academy of Sciences, Beijing 100190, People's Republic of China*

[3]*Department of Physics and Astronomy, Iowa State University, Ames, IA 50011, USA*

[4]*Department of Chemistry, Iowa State University, Ames, IA 50011, USA*

[5]*College of Chemistry, Beijing Normal University, Beijing 100875, People's Republic of China*

*Corresponding author: gangwang@iphy.ac.cn

ABSTRACT

Nitridoferrates containing monovalent iron ions are a class of materials of recent interest as potentially novel magnetic materials. Aiming at the exploration of nitridoferrates of calcium, we report the single crystal growth from Ca flux and crystal structure of the first member (n = 2) of a series of inverse Ruddlesden-Popper nitrides with a general formula of $A_{n-1}A'_2B_nX_{3n+1}$, where A = Li/Fe, A' = Te, B = N, and X = Ca. Single crystal X-ray diffraction analyses indicate the crystal with a composition of $Ca_7(Li_{0.32(1)}Fe_{0.68(1)})Te_2N_2$ and the tetragonal space group *I*4/*mmm* (*a* =

4.7884(1) Å, *c* = 25.3723(4) Å, Z = 2). The structure features alternately stacking NaCl-type A'X slabs and the perovskite-type ABX_3 slabs along the *c* axis. The Li/Fe atoms are located in cuboctahedral cavities surrounded by eight Ca_6N octahedra in the ABX_3 slab. This work demonstrates the viability of the Ca-rich flux as a suitable solvent for the exploration of new complex nitrides with interesting crystal structure and properties.

KEYWORDS

Nitrides; crystal growth; flux; crystal structure; Ruddlesden-Popper phase

1. Introduction

Binary nitride materials have attracted strong interest in both science and technology for their properties over the past decades. GaN and its III-V solid solutions are semiconductors widely used for the light emitting diode, laser diode, photodetector, and sensor application [1-5]. NbN, ZrN, and HfN are well known superconductors with relatively high superconducting transition temperatures for conventional superconductors [6-8]. Hexagonal BN is a good lubricant over a wide temperature range and a two-dimensional (2D) material offering a remarkable opportunity for advanced 2D devices [9,10]. Cubic BN and wurtzite BN are reported to have a hardness comparable to diamond [11,12].

More recently, interest in complex nitrides, like ternary and quaternary nitrides, has increased due to their specific properties [13]. Among complex nitrides, nitridoferrates of alkaline and alkaline earth metals, containing monovalent iron have attracted specific attention. Up to now, several nitridoferrates featuring one-dimensional (1D) N-(Li/Fe)-N chains, such as $Li_2[(Li_{1-x}Fe_x)N]$ [14,15], $CaLi_2[(Li_{1-x}Fe_x)N]_2$ [16], $SrLi_2[(Li_{1-x}Fex)N]_2$ [16], $Ca_2\{Li[(Li_{1-x}Fe_x)N_2]\}$ [17], and $Li_2Sr[Li_{1-x}Fe_xN]_2$ [18] have been reported. $Li_2[(Li_{1-x}Fe_x)N]$ [15] and $Li_2Sr[Li_{1-x}Fe_xN]_2$ [18] have

remarkable magnetic anisotropy and coercivity, which are desired for functional magnetic materials. Unlike the infinite N-(Li/Fe)-N chains, discrete N-(Li/Fe)-N linear blocks surrounded by Ca ion were discovered in the newly synthesized $Ca_6(Li_{1-x}Fe_x)Te_2N_3$ [19,20], which demonstrates the variety of possible coordination environments for the (Li/Fe)-N units.

Compared with their oxide counterparts, the growth and study of complex nitrides are difficult. Elemental nitrogen usually forms the diatomic molecule N_2 which has a strong covalent triple bond. The transition from atomic N to a N^{-3} anion needs to overcome a high energy barrier. Many of the nitrides are metastable phases and easily decompose. On one hand, these issues contribute to the challenge of synthesising nitride materials. On the other hand, this situation offers a vast unexplored territory and creates excellent opportunities to discover new nitride materials with interesting crystal structures and properties by developing suitable synthetic methods to overcome these obstacles.

Tremendous efforts have been devoted to preparing nitrides by solid-state reaction [21], ammonolysis [22], solid-state metathesis [23,24], vapour deposition [25], carbothermal reduction [26], reactive sputtering [27], precursor decomposition [28], solvothermal process [29], and solution growth [30,31]. The solution growth method utilises low melting point metals, such as alkaline metals or alkaline earth metals, as flux, dissolves reactants and facilitates reactions by attenuating the energy barrier for breaking the N-N bonding. Na, Li, and Ca flux have been successfully used to grow GaN single crystal [32-37], as well as other nitrides [31]. As such, the viability of alkaline metal and alkaline earth metal fluxes should definitely not be limited to the single crystal growth of binary nitrides.

Nitrogen is highly soluble in Ca [38], which also has a moderately high melting point 842 °C. The eutectic point of Ca-Ca_3N_2 is determined to be at 1.94 at.% N and 814 °C [39]. As such, Ca-rich

flux is postulated to be a suitable solvent for the exploration of complex nitrides of calcium. Here we report the discovery of an inversed Ruddlesden-Popper (RP) nitride $Ca_7(Li_{1-x}Fe_x)Te_2N_2$ with x = 0.68(1) grown by Ca flux. It crystallises in the tetragonal space group *I*4/*mmm* and contains a Li/Fe mixed site inside the cuboctahedral cavities defined by Ca_6N octahedra.

2. Experimental section

$Ca_7(Li_{1-x}Fe_x)Te_2N_2$ single crystals were grown by the solution growth method out of Ca-rich flux. Distilled Ca pieces (> 99.9%, Material Preparation Center (MPC), Ames Laboratory), lithium foil (99.9%, Alfa Aesar), tellurium (99.999%, Alfa Aesar), iron (99.99%, Alfa Aesar), and Ca_3N_2 (99%, Alfa Aesar) were weighed in the molar ratios of Ca:Li:Te:Fe:Ca_3N_2 = 7:1:1:0.1:1 and put inside a three-cap Ta crucible in an argon-filled glovebox [31]. The Ta crucible was sealed by arc welding under argon and loaded into an amorphous silica ampoule, which was sealed under roughly 0.2 atmosphere argon to prevent the oxidisation of Ta during the growth process. The growth ampoule was heated over 3 hours to 450 °C, held for 3 hours to melt tellurium and to react the elements, then heated over 12 hours to 1100 °C, held at this temperature for 4 hours, slowly cooled to 875 °C over 74 hours, and finally the assembly was decanted in a centrifuge to separate crystals from the remaining liquid. The $Ca_7(Li_{1-x}Fe_x)Te_2N_2$ crystals grow as rods with diameters ranging from several tens microns to millimeters and of lengths up to 7 mm, see Fig. 1. Single crystals of $Ca_7(Li_{1-x}Fe_x)Te_2N_2$ are very air sensitive and degrade within a few minutes in air. Besides $Ca_7(Li_{1-x}Fe_x)Te_2N_2$, CaTe was found as a byproduct.

Small $Ca_7(Li_{1-x}Fe_x)Te_2N_2$ pieces were selected under a microscope in a nitrogen-filled glovebox and sealed in quartz capillaries. Single-crystal X-ray diffraction data were collected at room temperature using a Bruker APEX II diffractometer equipped with a CCD area detector with Mo

Kα radiation. Refinements of the diffraction data were performed using the SHELXTL package [40].

The chemical compositions of $Ca_7(Li_{1-x}Fe_x)Te_2N_2$ single crystals were determined using a Bruker Aurora Elite Inductively Coupled Plasma Mass Spectrometer (ICP–MS) without collision gas. Samples were dissolved in 1% nitric acid, 1% hydrochloric acid solutions. The total mass of solute ranged from 0.6 mg to 3.4 mg, with a final sample solution concentration of 500 ppb. The isotopes analyzed were $^{7}Li^{+}$, $^{42}Ca^{+}$, $^{43}Ca^{+}$, $^{44}Ca^{+}$, $^{56}Fe^{+}$, $^{57}Fe^{+}$, and $^{125}Te^{+}$. External calibration curves of net signal vs. concentration were created using standard concentrations of 20, 200, and 2000 ppb. The molar ratios of (Li+Fe)/Ca and Li/Fe were determined as 0.147 and 0.471, respectively. The [(standard deviation/mean result) * 100] (%RSD) of the solution concentration in ppb for Li, Fe, and Ca are 1.25, 0.08, and 0.79, respectively.

The isothermal magnetization of $Ca_7(Li_{1-x}Fe_x)Te_2N_2$ was measured as a function of magnetic fields (up to ± 5 T) that were applied parallel and perpendicular to the rod at 5 K and 300 K. No apparent magnetic anisotropy between the two measured directions was observed. The saturated magnetic moments for both directions are about 0.02 μ_B/Fe, likely a result of impurity. We tried to measure the resistance of $Ca_7(Li_{1-x}Fe_x)Te_2N_2$ crystals by multimeter or making contacts using silver paint in the nitrogen-filled glovebox. In both cases, the resistance (sample and/or contacts) was too large to be measured.

3. Results and discussion

The crystal structure was determined by a direct method in the tetragonal structure with space group *I*4/*mmm*, in which the five independent metal sites were identified. Atomic assignments were made on the basis of peak intensities and bond distances to neighboring atoms. Subsequent difference Fourier map yield the N site. The final refinement with anisotropic displacement

parameters yielded a formula of $Ca_7(Li_{0.32(1)}Fe_{0.68(1)})Te_2N_2$. This proportion is consistent with the chemical composition determined by ICP–MS, which yielded a molar ratio of (Li+Fe)/Ca~0.147. Representative crystallographic data of the structural refinement are listed in Tables 1, 2, and 3.

As shown in Fig. 2(a), the structure of $Ca_7(Li_{0.32(1)}Fe_{0.68(1)})Te_2N_2$ manifest nitrogen centered Ca_6 octahedra, defined by four Ca1 atoms on the waist, and one Ca2 atom capping on the top and one Ca3 capping on the bottom. The Ca_6N octahedra are slightly distorted along *c*-axis, as indicated by the bond distance of d_{N-Ca2} = 2.325(3) Å and d_{N-Ca3} = 2.495(3) Å (see Table 3). These Ca-N distances of 2.325(3) Å, 2.4055(3) Å (d_{N-Ca1}), and 2.495(3) Å are within the range of reported Ca-N bond lengths for Ca_3N_2 (2.46 Å), $Ca_{11}N_8$ (2.308-2.900 Å), and Ca_2N (2.4426(4) Å) [41-43]. All Ca1 and Ca3 atoms are shared by neighboring octahedra to form 2D perovskite-type ABX_3 slabs, which are stacked along *c*-axis and separated by the more electronegative Te atoms. The Li/Fe atoms are located at the centers of cuboctahedral cavities in the perovskite layers, shown in Fig. 3(a). The (Li/Fe)-Ca distances are 3.2930(4)-3.3859(1) Å, within the range of Ca-Li and Ce-Fe distances commonly observed in intermetallics, e.g., $d_{Ca\text{-}Li}$ = 3.672 Å in Laves phase $CaLi_2$ [44] and $d_{Ca\text{-}Fe}$ = 3.219(1) Å in $CaFe_2Si_2$ [45]. The Te atoms in $Ca_7(Li_{0.32(1)}Fe_{0.68(1)})Te_2N_2$ are located between neighboring perovskites slabs; each has nine neighboring Ca atoms in its first coordinating sphere, shown in Figure 3(b).

Simply judging from the formula of $Ca_7(Li_{0.32(1)}Fe_{0.68(1)})Te_2N_2$, the title 7-1-2-2 phase seems to have a certain underpinned relationship with $Ca_6Li_{0.48}Fe_{0.52}Te_2N_3$ [19], or in short, 6-1-2-3 phase. However, their differences are remarkable: (1) there are two sets of N atoms in the 6-1-2-3 structure, one with octahedral coordination of six calcium atoms and the other with five calcium and one Li/Fe atoms, as shown in Fig. 2(b). Noteworthy is that Fe in the 6-1-2-3 phase can be considered as a cationic atom with a rare formal charge of +1 (d^6s^1 configuration), as confirmed

by susceptibility data and theory calculations [19]. Yet the same is not true for the 7-1-2-2 phase, which in fact is a metallic phase. (2) The Li/Fe-Li/Fe separation in the 6-1-2-3 phase is *c*/2 = 3.36 Å [19]. However, each Li/Fe in the 6-1-2-3 structure has direct bonding interaction with two electronegative N atoms with a distance of 1.86 Å. This could yield Fe-N-Fe super-exchange interactions as indicated by susceptibility data [19]. In contrast, Li/Fe in perovskite-type layer of the 7-1-2-2 phase is surrounded by 12 Ca atoms and no direct Li/Fe-N bonding exists as the separation is 4.7884(1) Å. Therefore, this material likely does not show strong magnetic response because of an expected electron delocalisation in the Ca_3N(Li/Fe) perovskite slab with intermetallic nature. In other words, the local region in the perovskite slabs is in fact dominated by homoatomic Ca-Ca and heteroatomic Ca-Li/Fe metallic bonding interactions. Although susceptibility and resistance data for $Ca_7(Li_{0.32(1)}Fe_{0.68(1)})Te_2N_2$ are not available, metallic luster is seen for the title crystals (cf. Figure 1).

In fact, the present 7-1-2-2 structure can be considered as the first member (n = 2) of an inverse RP phase, with a general formula of $A_{n-1}A'_2B_nX_{3n+1}$, here A = Li/Fe, A' = Te, B = N, and X = Ca. This type structure features alternately stacking NaCl-type A'X slabs and the perovskite-type ABX_3 slabs along the long axis. With this formula in hand, a series of new phases in the same system could be designed and to be synthesized by stoichiometric solid-state reactions, e.g., Ca_4Te_2N (n = 1) and $Ca_{10}(Li_{1-x}Fe_x)_2Te_2N_3$ (n = 3).

4. Conclusions

A novel inverse RP nitride $Ca_7(Li_{1-x}Fe_x)Te_2N_2$ with x = 0.68(1) was successfully grown from Ca flux. The single-crystal XRD indicates that it crystallizes in the tetragonal space group *I*4/*mmm* and contains Li/Fe ions located in cuboctahedral cavities in the perovskite-type layers formed by

Ca_6N octahedra. This work demonstrates the viability of Ca flux to crystallize new complex nitride, and predicts the existence of a series of new inversed RP phases in the title system.

Supporting Information

The following file is available free of charge.

Crystallographic Information Files (CIFs)

Acknowledgements

We would like to thank T. Kong, W. Straszheim, and U. S. Kaluarachchi for useful discussions and experimental assistance.

Disclosure statement

No potential conflict of interests was reported by the authors.

Funding

This work was supported by the U.S. Department of Energy, Office of Basic Energy Science, Division of Materials Sciences and Engineering. The research was performed at the Ames Laboratory. Ames Laboratory is operated for the U.S. Department of Energy by Iowa State University under Contract No. DE-AC02-07CH11358. G. Wang was supported by the National Natural Science Foundation of China (Grant Nos. 51572291 and 5132211), the National Key Research and Development Program of China (Grant No. 2017YFA0302902), and the China Scholarship Council. SM was supported by the Gordon and Betty Moore Foundations EPiQS Initiative through Grant GBMF4411. The ICP–MS device was originally provided by Bruker, presently Analytik Jena.

References

[1] S. Strite and H. Morkoç, *GaN, AlN, and InN: A review*, J. Vac. Sci. Tech. B 10 (1992), pp. 1237-1266.

[2] H. Morkoç, S. Strite, G.B. Gao, M.E. Lin, B. Sverdlov, and M. Burns, *Large-band-gap SiC, III-V nitride, and II-VI ZnSe-based semiconductor device technologies*, J. Appl. Phys. 76 (1994), pp. 1363-1398.

[3] S. Nakamura, M. Senoh, S.-I. Nagahama, N. Iwasa, T. Yamada, T. Matsushita, H. Kiyoku, and Y. Sugimoto, *InGaN-based multi-quantum-well-structure laser diodes*, Jpn. J. Appl. Phys., 35 (1996), pp. L74-L76.

[4] F.A. Ponce and D.P. Bour, *Nitride-based semiconductors for blue and green light-emitting devices*, Nature 386 (1997), pp. 351-359.

[5] O. Ambacher, *Growth and applications of Group III-nitrides*, J. Phys. D: Appl. Phys. 31 (1998), pp. 2653-2710.

[6] B.T. Matthlas and J.K. Hulm, *A search for new superconducting compounds*, Phys. Rev. 87 (1952), pp. 799-806.

[7] B.T. Matthlas, *Transition temperatures of superconductors*, Phys. Rev. 92 (1953), pp. 874-876.

[8] X.-J. Chen, V.V. Struzhkin, Z.G. Wu, M. Somayazulu, J. Qian, S. Kung, A.N. Christensen, Y.S. Zhao, R.E. Cohen, H.-K. Mao, and R.J. Hemley, *Hard superconducting nitrides*, Proc. Natl. Acad. Sci. USA 102 (2005), pp. 3198-3201.

[9] R. Haubner, M. Wilhelm, R. Weissenbacher, and B. Lux, *In Book Series in Structure and Bonding, volume 102: High Performance Non-Oxide Ceramics II*, Springer, Berlin, 2002, Chap. 1, pp. 1-45.

[10] L. Song, L.J. Ci, H. Lu, P.B. Sorokin, C.H. Jin, J. Ni, A.G. Kvashnin, D.G. Kvashnin, J. Lou, B.I. Yakobson, and P.M. Ajayan, *Large scale growth and characterization of atomic hexagonal boron nitride layers*, Nano Lett. 10 (2010), pp. 3209-3215.

[11] S.N. Monteiroa, A.L.D. Skuryb, M.G. Azevedob, and G.S. Bobrovnitchiib, *Cubic boron nitride competing with diamond as a superhard engineering material–an overview*, J. Mater. Res. Technol. 2 (2013), pp. 68-74.

[12] Z.C. Pan, H. Sun, Y. Zhang, and C.F. Chen, *Harder than diamond: Superior indentation strength of wurtzite BN and lonsdaleite*, Phys. Rev. Lett. 102 (2009), pp. 055503.

[13] R. Kniep, *Ternary and quaternary metal nitrides: A new challenge for solid state chemistry*, Pure Appl. Chem. 69 (1997), pp. 185-191.

[14] J. Klatyk and R. Kniep, *Crystal structure of dilithium (nitridolithiate/ferrate(I)), $Li_2((Li_{1-x}Fe_x)N)$ x = 0.63*, Z. Kristallogr. 214 (1999), pp. 447-448.

[15] A. Jesche, R.W. McCallum, S. Thimmaiah, J.L. Jacobs, V. Taufour, A. Kreyssig, R.S. Houk, S.L. Bud'ko, and P.C. Canfield, *Giant magnetic anisotropy and tunneling of the magnetization in $Li_2(Li_{1-x}Fe_x)N$*, Nature Commun. 5 (2014), pp. 3333.

[16] J. Klatyk and R. Kniep, *Crystal structure of alkaline earth dilithium bis(nitridolithiate/ferrates(I)), $CaLi_2[(Li_{1-x}Fe_x)N]_2$, x = 0.30 and $SrLi_2[(Li_{1-x}Fe_x)N]_2$, x = 0.46*, Z. Kristallogr. 214 (1999), pp. 449-450.

[17] J. Klatyk and R. Kniep, *Crystal structure of dicalcium (dinitridolithiate/ferrate(I)), $Ca_2\{Li[(Li_{1-x}Fe_x)N_2]\}$, x = 0.82*, Z. Kristallogr. 214 (1999), pp. 451-452.

[18] P. Höhn, T.J. Ball, M. Fix, Y. Prots, and A. Jesche, *Single crystal growth and anisotropic magnetic properties of $Li_2Sr[Li_{1-x}Fe_xN]_2$*, Inorganics 4 (2016), pp. 42.

[19] M.J. Dickman and S.E. Latturner, *Metal nitrides grown from Ca/Li Flux: $Ca_6Te_3N_2$ and new nitridoferrate(I) $Ca_6(Li_xFe_{1-x})Te_2N_3$*, J. Am. Chem. Soc. 138 (2016), pp. 10636-10644.

[20] X.-W. Yan, Z.B. Huang, C.F. Zhang, M. Gao, L. Chen, G.H. Zhong, and H.-Q. Lin, *Magnetic moment and spin state transition on rare monovalent iron ion in nitridoferrate $Ca_6Li_{0.5}Fe_{0.5}Te_2N_3$*, J. Mater. Chem. C 5 (2017), pp. 733-737.

[21] D.H. Gregory, *Structural families in nitride chemistry*, J. Chem. Soc., Dalton Trans. 3 (1999), pp. 259-270.

[22] P.S. Herle, M.S. Hegde, N.Y. Vasathacharya, S. Philip, M.V. Rama Rao, and T. Sripathi, *Synthesis of TiN, VN, and CrN from ammonolysis of TiS_2, VS_2, and Cr_2S_3*, J. Solid State Chem. 134 (1997), pp. 120-127.

[23] E.G. Gillan and R.B. Kaner, *Rapid solid-state synthesis of refractory nitrides*, Inorg. Chem., 33 (1994), pp. 5693-5700.

[24] B. Song, J.K. Jian, G. Wang, M. Lei, Y.P. Xu, and X.L. Chen, *Facile and general route to nitrides by a modified solid-state metathesis pathway*, Chem. Mater. 19 (2007), pp. 1497-1502.

[25] S.C. Jain, M. Willander, J. Narayan, and R. Van Overstraeten, *III–nitrides: Growth, characterization, and properties*, J. Appl. Phys. 87 (2000), pp. 965-1006.

[26] H.Z. Zhao, M. Lei, X.A. Yang, J.K. Jian, and X.L. Chen, *Route to GaN and VN assisted by carbothermal reduction process*, J. Am. Chem. Soc. 127 (2005), pp. 15722-15723.

[27] J. Pelleg. L.Z. Zevin, and S. Lungo, *Reactive-sputter-deposited TiN films on glass substrates*, Thin Solid Films 197 (1991), pp. 117-128.

[28] P. Gibart, *Metal organic vapour phase epitaxy of GaN and lateral overgrowth*, Rep. Prog. Phys. 67 (2004), pp. 667-715.

[29] B.G. Wang and M.J. Callahan, *Ammonothermal synthesis of III-nitride crystals*, Crystal Growth Des. 6 (2006), pp. 1227-1246.

[30] E. Meissner, S. Hussy, and J. Friedrich, *In Book Series in Springer Series in Materials Science, Volume 133: Technology of Gallium Nitride Crystal Growth*, Springer, Heidelberg, Dordrecht, London, New York, 2010, Chap. 12, pp. 245-273.

[31] A. Jesche and P.C. Canfield, *Single crystal growth from light, volatile and reactive materials using lithium and calcium flux*, Philos. Mag. 94 (2014), pp. 2372-2402.

[32] H. Yamane, M. Shimada, S.J. Clarke, and F.J. DiSalvo, *Preparation of GaN single crystals using a Na flux*, Chem. Mater. 9 (1997), pp. 413-416.

[33] Y.T. Song, W.J. Wang, W.X. Yuan, X. Wu, and X.L. Chen, *Bulk GaN single crystals: Growth conditions by flux method*, J. Cryst. Growth 247 (2003), pp. 275-278.

[34] G. Wang, J.K. Jian, W.X. Yuan, and X.L. Chen, *Growth of GaN single crystals using Ca-Li_3N composite flux*, Cryst. Growth Des. 6 (2006), pp. 1157-1160.

[35] J.K. Jian, G.Wang, C. Wang, W.X. Yuan, and X.L. Chen, *GaN single crystals grown under moderate nitrogen pressure by a new flux: Ca_3N_2*, J. Cryst. Growth 291 (2006), pp. 72-76.

[36] G. Wang, W.X. Yuan, J.K. Jian, H.Q. Bao, J.F. Wang, X.L. Chen, and J.K. Liang, *Growth of GaN single crystals by Ca_3N_2 flux*, Scripta Mater. 58 (2008), pp. 319-322.

[37] G. Wang and X.L. Chen, *Single-crystal growth: From new borates to industrial semiconductors*, Phys. Status Solidi A 207 (2010), pp. 2757-2768.

[38] V. P. Itkin and C. B.Alcock, *CaN phase diagram, In ASM Alloy Phase Diagrams Center*, P. Villars, H. Okamoto, and K. Cenzual, eds. ASM International, Materials Park, OH, 1990. Available at http://www1.asminternational.org/AsmEnterprise/APD

[39] G. Wang, W.X. Yuan, J.F. Wang, X. Zhao, J.K. Jian, and X.L. Chen, *Thermodynamic assessment of the Ca–Ca_3N_2 system*, Mater. Lett. 61 (2007), pp. 2266-2269.

[40] G.M. Sheldrick, *SHELXL-97. Program for the Solution of Crystal Structures*, University of Göttingen, Göttingen, Germany 1997.

[41] P.Y. Laurent, J. Lang, and E.M.T. Le Bihan, *Structure du nitrure de calcium α*, Acta Cryst. B 24 (1968), pp. 494-499.

[42] P.Y. Laurent, J. Lang, and E.M.T. Le Bihan, *Structure d'un nouveau nitrure de calcium: $Ca_{11}N_8$*, Acta Cryst. B 25 (1969), pp. 199-203.

[43] D.H. Gregory, A. Bowman, C.F. Baker, and D.P. Weston, *Dicalcium nitride, Ca_2N-A 2D "excess electron" compound; synthetic routes and crystal chemistry*, J. Mater. Chem. 10 (2010), pp. 1635-1641.

[44] D. Fischer and M. Jansen, *Eine neue modifikation der Laves-phase $CaLi_2$*, Z. Anorg. Allg. Chem. 629 (2003), pp. 1934-1936.

[45] V. Hlukhyy, A. Hoffmann, and T.F. Fäessler, *Synthesis, structure and chemical bonding of $CaFe_{2-x}Rh_xSi_2$ (x = 0, 1.32, and 2) and $ScCo_2Si_2$*, J. Solid State Chem. 203 (2013), 232-239.

Table 1. Crystal structure data of $Ca_7(Li_{0.32(1)}Fe_{0.68(1)})Te_2N_2$ obtained by structural refinement.

Empirical formula	$Ca_7(Li_{0.32(1)}Fe_{0.68(1)})Te_2N_2$
Space group, Z	*I*4/*mmm*, 2
Unit cell (Å)	*a* = 4.7884(1)
	c = 25.3723(4)
Vol. (Å^3)	*V* = 581.76(3)
d_{cal} (g/cm^3)	3.448
Reflections collected/R_{int}	8804/0.0302
Data/restraints/parameters	308/0/20
Goodness-of-fit on F^2	1.147
R1/wR2 [I>2σ(I)]	0.0118/0.0302
(all data)	0.0127/0.0305
Peak and hole (e.Å^{-3})	0.419/-0.517

Table 2. The refined atomic positions and equivalent isotropic displacement parameters for $Ca_7(Li_{0.32(1)}Fe_{0.68(1)})Te_2N_2$.

Atom	Wyck.	Site	S.O.F.	*x*	*y*	*z*	U_{eq} (Å^2)
Te	4e	4mm		0	0	0.1845(1)	0.013(1)
Li/Fe	2a	4/mmm	0.680/0.320(5)	0	0	0	0.007(1)
Ca1	8g	2mm		0	0.5	0.08912(1)	0.013(1)
Ca2	4e	4mm		0	0	0.3100(1)	0.017(1)
Ca3	2b	4/mmm		0	0	1/2	0.016(1)
N	4e	4mm		0	0	0.4017(1)	0.007(1)

Table 3. Environments and bond distances around Te, Li/Fe, and N atoms in $Ca_7(Li_{0.32(1)}Fe_{0.68(1)})Te_2N_2$, and selected interatomic distances between Ca atoms.

Bond	Distance (Å)	Bond	Distance (Å)	Bond	Distance (Å)
Te-Ca1 x 4	3.4032(5)	Li/Fe-Ca1 x 4	3.2930(4)	N-Ca1 x 4	2.4055(3)
Te-Ca2 x 1	3.1862(9)	Li/Fe-Ca1 x 4	3.2933(4)	N-Ca2 x 1	2.325(3)
Te-Ca2 x 4	3.3888(1)	Li/Fe-Ca3 x 4	3.3859(1)	N-Ca3 x 1	2.495(3)
Ca1-Ca1	3.3859(1)	Ca1-Ca2	3.5044(8)	Ca1-Ca3	3.2934(4)
		Ca1-Ca2	3.5040(8)	Ca1-Ca3	3.2930(4)

Figure 1. Optical photograph of $Ca_7(Li_{1-x}Fe_x)Te_2N_2$ single crystals.

Figure 2. Crystal structures for (a) $Ca_7(Li_{0.32(1)}Fe_{0.68(1)})Te_2N_2$ and (b) $Ca_6Li_{0.48}Fe_{0.52}Te_2N_3$.

Figure 3. Environments of (a) Li/Fe and (b) Te in $Ca_7(Li_{0.32(1)}Fe_{0.68(1)})Te_2N_2$. Large spheres denote Ca atoms, with atomic sequence marked as given in Table 2. Small and middle spheres denote Li/Fe and Te atoms, respectively. Representative bond distances are also marked.

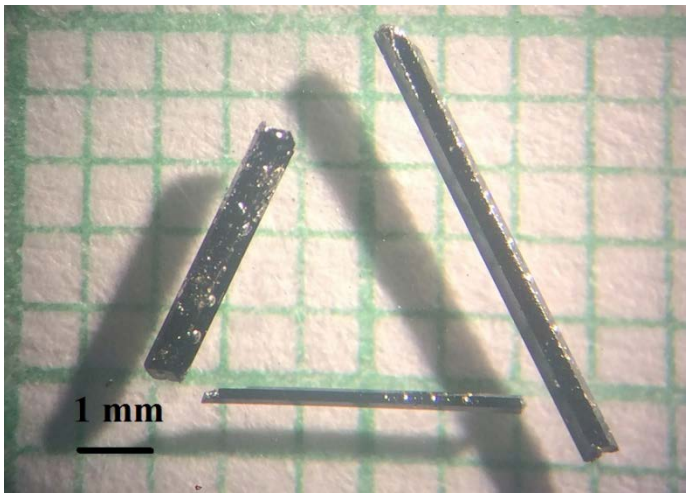
1 mm

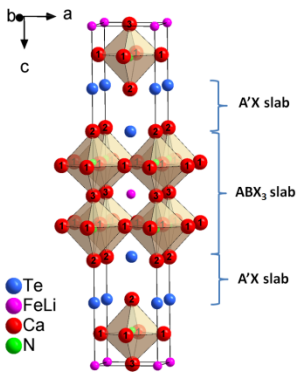

(a)

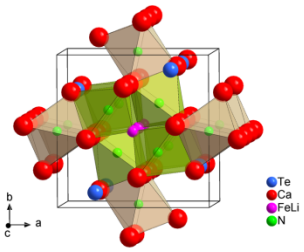

(b)

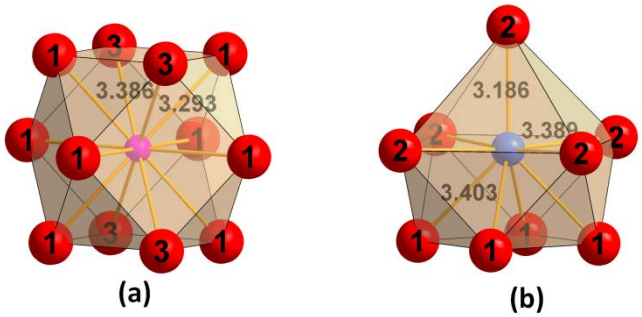
3.386
3.293
3.186
3.389
3.403
(a)
(b)